

# Anti-HER2 VHH Targeted Magnetoliposome for Intelligent Magnetic Resonance Imaging of Breast Cancer Cells

SEPIDEH KHALEGI,<sup>1</sup> FATEMEH RAHBARIZADEH,<sup>1</sup> DAVOUD AHMADVAND,<sup>2</sup>  
and HAMID REZA MADAAH HOSSEINI<sup>3</sup>

<sup>1</sup>Department of Medical Biotechnology, Faculty of Medical Sciences, Tarbiat Modares University, P.O. BOX. 14115-331, Tehran, Iran; <sup>2</sup>School of Allied Medical Sciences, Iran University of Medical Sciences, Tehran, Iran; and <sup>3</sup>Materials Science and Engineering Department, Sharif University of Technology, Azadi Avenue, P.O. BOX. 11155-9466, Tehran, Iran

(Received 7 August 2016; accepted 10 February 2017; published online 28 February 2017)

Associate Editor Partha Roy oversaw the review of this article.

**Abstract**—The combination of liposomes with magnetic nanoparticles, because of their strong effect on T2 relaxation can open new ways in the innovative cancer therapy and diagnosis. In order to design an intelligent contrast agent in MRI, we chose anti-HER2 nanobody the smallest fully functional antigen-binding fragments evolved from the variable domain, the VHH, of a camel heavy chain-only antibody. These targeted magnetoliposomes bind to the HER2 antigen which is highly expressed on breast and ovarian cancer cells so reducing the side effects as well as increasing image contrast and effectiveness. Cellular iron uptake analysis and *in vitro* MRI of HER2 positive cells incubated with targeted nanoparticles show specific cell targeting. *In vitro* MRI shows even at the lowest density (200 Cells/ $\mu$ l), dark spots corresponding to labeled cells which were still detectable. These results suggest that this new type of nanoparticles could be effective antigen-targeted contrast agents for molecular imaging.

**Keywords**—Magnetoliposome, Specific cell targeting, VHH, Molecular imaging, Breast cancer.

## INTRODUCTION

In the last few years, molecular imaging has emerged as a new area aiming at a minimally invasive visualization of expression and function of bioactive molecules at the molecular, sub-cellular, or cellular level.<sup>1,10</sup> Recently, there is a great deal of interest in the development of inorganic nanoparticles (NPs) such as quantum dots, carbon nanotubes, gold, or iron oxide for enormous applications in biomedical fields.<sup>22</sup> Several systems have been designed and tested to accom-

modate paramagnetic or superparamagnetic materials and to act as highly efficient contrast agents (CA) for magnetic resonance imaging (MRI).<sup>20,28</sup> As MRI is inherently a rather insensitive technique, high contrast generation and the ability to monitor the cells for longer times require that the cells are loaded with high amounts of iron oxide nanoparticles (IONPs). This has stimulated the development of novel IONP types to reduce IONPs induced toxicity while maintaining or even augmenting the magnetic contrast. Among these attempts, coating USPIOs with phospholipids that generally referred to as magnetoliposomes (MLs) can stable NPs for their successful experimental use in addition liposomes favorably ameliorates their pharmacokinetics, resulting in improved CAs effects by increasing the quantity of agents in the tumor and significantly reducing non-specific toxicities to normal cells.<sup>24</sup> MLs are an ideal platform as CA due to their strong effect on T2 relaxation. Moreover, modifying the surface of nanoparticles with polyethylene glycol (PEG) prolongs circulation time in blood and reduces reticuloendothelial system uptake.<sup>11</sup> Molecular targeting of the nanoparticles to cancer cells *via* antibodies to their cell surface markers may further enhance the accumulation of the nanoparticles in tumors, prolong their retention, and potentially allow the use of lower nanoparticle dosages.<sup>26</sup> In several studies there is significant interest in the utilization of VHHs because of unique characterization (their unique properties of size, intrinsic stability, and ease of manufacture<sup>12</sup>) and impressive potential for therapy and *in vivo* diagnosis.<sup>8,17,18</sup> Because of the pro-tumorigenic properties of human epidermal growth factor receptor 2 (HER2), such as the strong catalytic kinase activity, the extracellular accessibility, the high expression and association with poor prognosis, HER2 has been identified as

Address correspondence to Fatemeh Rahbarizadeh, Department of Medical Biotechnology, Faculty of Medical Sciences, Tarbiat Modares University, P.O. BOX. 14115-331, Tehran, Iran. Electronic mail: rahbarif@modares.ac.ir

a promising target for antibody-based therapy.<sup>7</sup> In one study, Oliveira *et al.* designed and prepared anti EGFR (EGa1) nanobody coupled to PEG-liposome in order to EGFR down regulation.<sup>13</sup> In another study, Rotman *et al.* prepared Two different formulations of GSH-PEG liposome containing 15 kDa amyloid beta binding llama single domain antibody fragments (VHH-pa2H) for Alzheimer's disease.<sup>15</sup> Up to now several VHHs were generated for imaging modalities (SPECT, optical, PET and ultrasound).<sup>4</sup> Fortunately, the exclusive physical properties of MLs along with VHH as targeting agent, enable them to serve as imaging probes for locating and diagnosing cancerous lesions.<sup>2</sup> Near 20 years ago, Shinkai *et al.* had prepared Antibody-conjugated MLs for targeting cancer cells for hyperthermia treatment.<sup>19</sup> In previous researches, no study has not been done yet in the surface engineering of MLs by nanobody moreover no assuming was done in the anti-HER2 VHH MLs cellular uptake and *in vitro* MRI on HER2 positive and HER2 negative breast cancer cell lines.

In this study, we developed targeted MLs by anti-HER2 VHH for the first time in order to intelligent MRI. With the purpose of this goal, at first we designed and targeted MLs by anti-HER2 VHH and Herceptin separately. In a comparative study, *in vitro* cell uptake and cytotoxicity of targeted MLs as well as non-targeted MLs were evaluated on HER2-positive, HER2-negative cancerous and normal breast cell lines. The capacity of targeted cell labeling strategy by HER2-based immunomagneto liposomes has been demonstrated *via* cellular iron uptake and *in vitro* MRI, as an efficient contrast agent for intelligent MRI.

## MATERIALS AND METHODS

### *Chemicals and Reagents*

1,2-Dipalmitoyl-sn-glycero-3-phosphocholine (DPPC), cholesterol, 1,2-distearoyl-sn-glycero-3-phosphoethanolamine-N-[methoxy(polyethylene glycol)-2000] (ammonium salt) (DSPE-mPEG(2000)) and 1,2-distearoyl-sn-glycero-3-phosphoethanolamine-N-[maleimide (polyethylene glycol)-2000] (ammonium salt) (DSPE-PEG(2000) maleimide) were purchased from Avanti polar lipids. USPIOs coated by dextran provided in (Biomaterial laboratory, Sharif University of Technology, Tehran, Iran). 3-(4,5-Dimethylthiazol-2-yl)-2,5-diphenyltetrazolium bromide (MTT) salt was bought from Sigma-Aldrich (St. Louis, USA).

### *Cell Culture Conditions*

BT-474 (HER2-overexpressing breast cancer cell line) and MDA-MB-231 (HER2 and estrogen receptor negative breast cancer cell line) were grown in RPMI-1640 (100 U/mL penicillin, 100 µg/mL streptomycin and 2 mM/L glutamine) with or without 10% FBS and SK-BR-3 (HER2-overexpressing breast cancer cell line), MCF-10A (human normal breast epithelial cell line) was cultured in the DMEM/F12 medium supplemented with 5% horse serum, 100 mg/mL EGF, 1 mg/mL hydrocortisone, 10 mg/mL insulin, 100 units/mL of penicillin and 100 mg/mL of streptomycin.

### *Preparation of MLs*

MLs were prepared from dextran-stabilized Fe<sub>3</sub>O<sub>4</sub>, using the classical film method following by extrusion. In brief, the lipids DPPC:cholesterol:DSPE-PEG2000:DSPE-PEG-mal in a molar ratio of 7:2.5:0.4:0.1 and in amounts required to obtain a final lipid concentration of 50 mg/mL, were dissolved in a mixture of chloroform and methanol (9:1, volume ratio) in a round-bottom flask and dried in a rotary evaporator under reduced pressure at 45 °C to form a thin film on the flask. After the complete removal of the chloroform, the lipid film was hydrated with the appropriate amount of the mixture of water and USPIO at 45 °C for 1 h. Multilamellar liposomes (MLV) were downsized to form unilamellar vesicles by extrusion (Avanti Polar Lipids, Inc.) with polycarbonate membranes (Avanti Polar Lipids, Inc.) with pore diameters of 100 nm 21 times at 45 °C.

### *Particle Characterization of Magnetoliposomes*

In MLs, the size, distribution and electrophoretic mobility of the particle size were determined by dynamic light scattering at 25 °C with a Zetasizer Nano ZS90 (Malvern, UK). MLs were diluted with PBS 10 mM until a concentration of approximately 0.2 g/L of magnetite. To avoid those MLs can settle due to the high density of the magnetite, the measurement was carried out with three different samples. To further determine the size of the MLs, transmission electron microscopy (TEM) was performed. Approximately 5 µL of MLs solution was placed on a carbon grid. Liquid was then removed from the carbon grid, and the grid was imaged on a Hitachi H-7500 TEM. Scanned images were then analyzed in Adobe® Image Ready™, version 3.0, to determine approximate diameters.

### Optimization of VHH Thiolation

In order to achieve conjugation of the biologically active VHH, the thiolation step of the VHH as well as the conjugation step to the particle surface is crucial for quality of the resulting nanoparticle. Therefore, at the beginning of the study a special focus was on the optimization of the thiolation procedure of the VHH under the aspect of an effective binding to particle surfaces. For the introduction of thiol groups several kinds of VHH/Truot mole ratios were used. The ratios of 1:1, 1:2, 1:3, 1:4, 1:5, 1:7.5, 1:10 and 1:15 were evaluated and the volume of the samples was adjusted to 3 mL with thiolation buffer (pH 8.3). The samples were incubated for 1 h at room temperature under constant shaking (600 rpm). The thiolation of Herceptin was based on the Steinhäuser *et al.* According to that study the reaction time for a standard protocol was fixed to 2 h at 50-fold molar excess of 2-iminothiolane.<sup>25</sup>

### Preparation of Anti-HER2 Targeted MLs

In order to conjugate thiolated VHH to liposomes, the buffer was exchanged with phosphate buffer by Amicon filter 30,000 Dalton and the pH was adjusted to 7.0. To optimize immune magnetoliposomes preparation, the samples were incubated for 1, 2, 3, and 24 h at 20 and 4 °C under constant and gentle shaking. In all samples, 50 mg liposome was added to 1.8 g/L VHH and the volume of the samples was adjusted to 1 mL with phosphate buffer (pH 7). With the purpose of Herceptin conjugation, the antibody thiolated with 50-fold molar excess of 2-iminothiolane for 2 h and the buffer was exchanged as described above. An aliquot (1 g/L) of thiolated Herceptin solution in phosphate buffer pH 7 were added to 50 mg liposome under constant gentle shaking at room temperature for 1 h and the volume of the samples was adjusted to 1 mL with phosphate buffer (pH 7). Conjugation was confirmed by SDS-PAGE followed by silver staining.<sup>27</sup>

### Stability Assessment of Anti-HER2 VHH Targeted Magnetoliposomes

To examine the stability of anti-HER2 VHH targeted MLs for *in vitro* experiments; the sizes and zeta potential of the MLs were measured during 4 weeks after sample preparation in several concentrations of FBS (Fetal Bovine Serum, 1, 5 and 10%). Every 1 week, aliquots (50  $\mu$ L) of the nanoparticle suspensions were analyzed for particle size and zeta potential changes respectively.

### Cell Viability and Metabolic Activity of Immunomagnetoliposomes

PrestoBlue™ Cell Viability Reagent is a ready-to-use reagent for rapidly evaluating the viability and proliferation of a wide range of cell types. For this purpose, BT-474, SK-BR-3, MCF10-A and MDA-MB-231 cell lines were seeded on 96-well microtiter plate at a density of  $4 \times 10^4$ ,  $3 \times 10^4$ ,  $2 \times 10^4$  and  $3 \times 10^4$  respectively, then incubated with MLs (200 and 400  $\mu$ g Fe/mL), liposomes (adjust to MLs) and magnetites coated by dextran (200 and 400  $\mu$ g Fe/mL). Presto blue assay was done according to the manufacturer's protocol. PrestoBlue™ reagent is a resazurin-based solution that functions as a cell viability indicator by using the reducing power of living cells to quantitatively measure the proliferation of cells. PrestoBlue™ reagent (PB) is quickly reduced by metabolically active cells, providing a quantitative measure of viability and cytotoxicity in as little as 10 min. After 24 h treatment of the cells with the samples, the cells were washed and incubated with PB reagent. The changes in cell viability were detected using both, fluorescence and absorbance spectroscopy. The absorbance was recorded at 570 nm after 2 h incubation of mentioned cells with PB reagent, whereas the fluorescence was read (excitation 570 nm; emission 610 nm) at recommended time of incubation (20 min and 2 h endpoint). The cell viability was expressed as a percentage relative to the non-treated cells.

### Visualization of Targeted MLs Uptake

Cellular uptake of iron oxide cores was visualized by light microscopy by using Prussian blue staining. The cells were seeded at a density of  $1 \times 10^4$  cells per well in 6-well plates that contained cover slips (3 mm diameter). After incubation for 8 h at 37 °C in a 5% CO<sub>2</sub> atmosphere, the medium was replaced with fresh complete medium that contained VHH-modified and Herceptin-modified MLs (concentration: 200  $\mu$ g Fe/mL). Cell staining was done according to Soenen *et al.*<sup>21</sup>

### Determination of Intracellular Iron Content

A quantitative colorimetric iron determination at 490 nm was used for studying cellular iron uptake. In accordance with De Cuyper *et al.*'s protocol.<sup>3</sup> After incubating the cells with targeted and non-targeted MLs, and subsequently removing the medium that contained the non internalized MLs, a mixture (28.8 mL) that consisted of TES buffer (16 mL, 5 mM,

pH 7.0), HCl (9.6 mL, 37%) and of HNO<sub>3</sub> (3.2 mL, 65%)<sup>21</sup> was applied to each well. To dissolve the colloidal Fe<sub>3</sub>O<sub>4</sub> cores, the plate was placed on a shaker and shaken at 1200 rpm at 37 °C for 2 h, then distilled water (51.5 mL) was added, followed by a 5:1 mixture (96 mL) of KOH (4 N), Tiron (0.25 M) and phosphate buffer (160 mL, 0.2 M, pH 9.5). After incubation for 15 min at room temperature, 100 µL of solution was transferred to a new ELISA plate then the absorbance was measured at 490 nm on the ELISA plate reader, and the iron uptake was determined by comparing the absorbance with that of untreated cells. A standard curve ranging from 0 to 100 mg/mL Fe<sup>+3</sup> was constructed by starting from a stock solution (1 mg/mL Fe<sup>+3</sup>). The absorbance was quantified by using this standard curve that covered the range of 0–100 mg/mL of Fe<sup>+3</sup>. To determine the average amount of iron per cell, the total iron concentration was divided by the total amount of protein (by Quick Start<sup>TM</sup> Bradford Protein Assay), which was then converted to the amount of iron per total cell number.

#### *Ex Vivo Imaging*

Several human breast cell lines (BT-474, SK-BR-3) and (MDA-MB-231, MCF10-A) were grown in 24-well plates at 60–70% confluence and then incubated with Herceptin, anti-HER2 VHH targeted MLs, non-targeted MLs and magnetite nanoparticles at 200 µg Fe/mL for 8 h. Cells were then washed three times with PBS, trypsinized, spun down by centrifugation and fixated in 4% glutaraldehyde for 20 min at room temperature (RT). Cells were then spun down again and dispersed in 100 µL PBS to make stock cell suspensions. Of this stock suspension, four dilutions were prepared in 100 µL of 1% agarose gel, leading to 1000, 500, 200 cells/µL and placed in 1.5 mL micro tubes. These tubes were further filled with 1.5% agarose gel and placed in a water block. As control, a tube filled completely with 1.5% agarose was taken. Upon solidification, the study was performed by 1.5 T GE MR Scanner at 25 °C with a 90 mm × 90 mm field of view (FOV), one acquisition and matrix size of 256 × 196 pixels and 5 mm slice thickness.

#### *Statistical Analysis*

The different experimental groups within the study were compared by using the MANOVA test. The comparisons between the pairs of groups were performed with the One Way ANOVA test. A probability of less than 0.05 ( $p < 0.05$ ) was used for statistical significance.

## RESULTS

### *Characterizations of the Nanosized Anti-HER2 Targeted MLs*

In order to confirm the physical characterization of MLs, several usual techniques were used. As prepared MLs [containing 45 g of magnetite/mol of phospholipid (PI)]<sup>9</sup> was brownish appearance and highly soluble in water. The number of USPIO particles in each liposome was calculated according to Soenen *et al.* For a Fe<sub>3</sub>O<sub>4</sub> content of 45 mg Fe<sub>3</sub>O<sub>4</sub>/mol PI, a theoretical number of 83 particles for a single ML were calculated, assuming spherical unilamellar vesicles of 100 ± 10 nm diameter and spherical 20 nm diameter Fe<sub>3</sub>O<sub>4</sub> cores. Figure 1 was obtained by TEM without staining the samples. The average size of non-targeted ML was 100 ± 10 nm and the zeta potential of 0.42 ± 0.3 mV near to inert. After surface modification with VHH an average size of 110 ± 10 nm with PI below 0.1 and a surface charge of -5 ± 0.5 mV were achieved. The negative zeta potential of anti-HER2 VHH-MLs can reduce nonspecific internalization. In compare with VHH, the Herceptin conjugation has no effect on surface charge of nanoparticles, these results confirmed by Steinhauser *et al* too.<sup>25</sup>

### *Optimization of Thiolation*

The free sulfhydryl groups are necessary for covalent conjugation to particle surface but these groups bear the risk of oxidative disulfide bridge formation leading to dimers or even higher oligomers of VHH. These by-products could affect the biological activity and thus were objectionable. The 1:1 or 1:2 VHH/Truait mole ratios were chose for conjugation because the aggregation was at least. After thiolation by Truait reagent, the amount of thiol groups were measured by disulfide building with 5,5'-dithiobis-(2-nitrobenzoic acid) or DTNB (Ellman's reagent). As could be expected at 1:1 or 1:2 VHH/Truait mole ratios the highest number of 1.2 ± 0.15 sulfhydryl groups per VHH was introduced. On the basis of our results the reaction time for a standard protocol should be set to 1 h at 1:2 VHH/Truait mole ratios. According to Steinhauser *et al* at 50-fold molar excess the highest number of 0.71 ± 0.15 sulfhydryl groups per Herceptin was introduced.

### *Preparation of Immunomagnetoliposomes*

The surface of the particles was PEGylated and activated by PEG-DSPE and Maleimide-PEG-DSPE respectively. The SEC analysis of the supernatants revealed, that the VHH was quantitatively bound to the



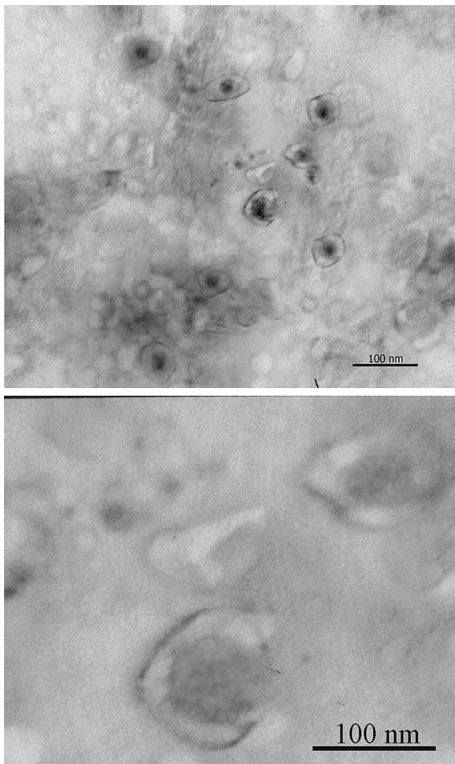


**FIGURE 1.** TEM image of MLs without staining. It shows the phospholipid bilayer surrounding the electron dense iron oxide cores.

nanoparticle surface by effective percent near to 70% (Fig. 2). Based on these results, in average 27  $\mu\text{g}$  nanobody were attached per mg nanoparticle which corresponds to 58 VHH molecules per nanoparticles. Because Herceptin is a monoclonal antibody with two antigen binding sites, in order to synthesis targeted MLs with the same number of antigen binding site, 65  $\mu\text{g}$  Herceptin were attached per mg nanoparticle which corresponds to nearly 30 Herceptin molecules per nanoparticles.

#### *Stability Assessment of Anti-HER2 VHH Targeted Magnetoliposomes*

To evaluate the influence of the FBS proteins on the nanoparticles size and zeta potential, several FBS concentrations were analyzed during 4 weeks in cell culture medium. The results obtained are given in Fig. 3. Because of negative charge on the surface of anti-HER2 VHH targeted MLs, the FBS proteins can have at least effects on the size and zeta potential of the nanoparticles (Figs. 3a, 3b). Furthermore the PEG on the magnetoliposome surface can reduce non covalent

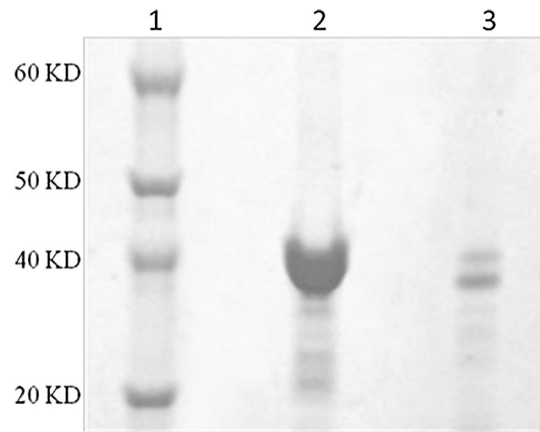


**FIGURE 2.** Confirm of conjugation of antibody and liposomes by coomassie blue and silver staining. The heavier band in compare to VHH band, represent the conjugation of VHH to the surface of magnetoliposomes. (1) Protein ladder. (2) Free VHH. (3) ML conjugates. (4) ML conjugates with silver staining.

connection and maintain the size and zeta potential of nanoparticles. The differences in size and zeta potentials of samples in different concentrations of FBS were not significant and these showed our nano particles have suitable stability even in 10% FBS during 4 weeks storage.

#### *Comparison of the Cytotoxicity of MLs Nanoparticles*

To compare the cellular toxicities of dextran coated USPIOs, MLs and iron oxide free vesicles, on cell viability of BT-474, SK-BR-3, MDA-MB-231 and MCF10-A, these cell lines were incubated with these nanoparticles, all containing the same phospholipid components and identical preparation process. As anticipated, there is no significant cytotoxicity among samples after 24 h (Fig. 4). The dextran coated magnetite, inert PEGylated magnetoliposomes and iron free vesicles have no considerable effects on cell viability. The results indicate that cell labeling at the non-toxic concentrations of  $\text{Fe}^{+3}$  indeed did not cause any acute toxicity.

#### *The Cellular Iron Uptake*

The uptake of MLs by BT-474, SK-BR-3 as HER2 positive breast cancer cell line and MDA-MB-231, MCF10-A as negative control was investigated by using VHH and Herceptin targeted, non-targeted MLs and magnetite. Figure 5 shows optical micrographs of Prussian blue stained cell lines that were incubated for

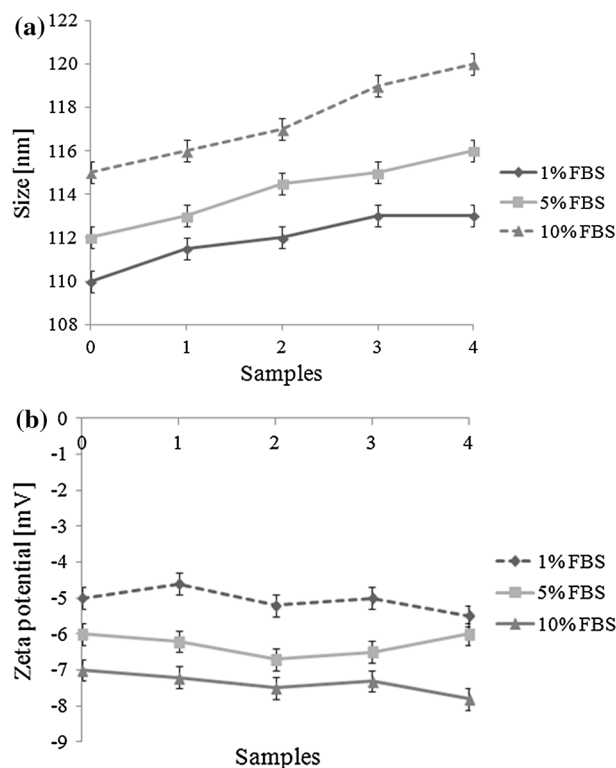


**FIGURE 3.** Storage stability of anti-HER2 targeted magnetoliposomes in cell culture medium plus 1, 5 and 10% FBS. Particle size (a) and zeta potential (b) were recorded over a time period of 4 weeks ( $n = 3$ ; mean  $\pm$  SD).

8 h with these three types of samples at a concentration of  $200 \mu\text{g Fe/mL}$ . When the cells were incubated with non-targeted MLs or magnetite only a few dark dots were seen, Figs. 5a and 5b, respectively. In contrast, when targeted MLs were used, the cells were heavily loaded with the ML colloids (Figs. 5c, 5d); this visual inspection showed that the amount of iron that was taken up per cell was quite variable. Quantitative data on the average iron oxide uptake per cell after 8 h incubation were obtained by a Prussian blue colorimetric assay determination (Fig. 6). The results clearly show that the cellular iron concentrations in targeted MLs are more than the non-targeted MLs or magnetite. In compare between anti-HER2 VHH and Herceptin, the Fig. 6 shows the anti-HER2 VHH MLs can effectively labeled HER2 positive cell lines in compare with Herceptin targeted MLs. Of course the cellular iron uptake is depend on cell line specificities, nanoparticle characterization and targeting agent traits, so the comparison between two kinds of targeting agents with different specificities is not logical. Obviously the VHHs with peculiar characteristics

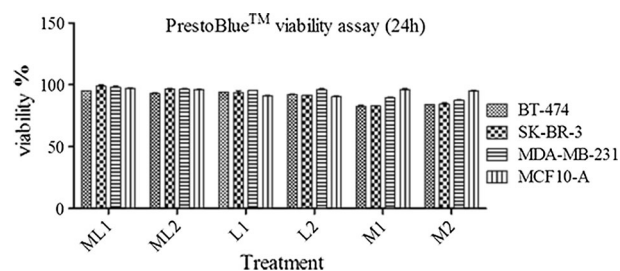


**FIGURE 4.** PrestoBlue™ Cell Viability assay. Cell viability assay for HER2 positive (SK-BR-3 and BT-474), HER2 negative (MDA-MB-231) and normal breast cell line (MCF10-A) incubated with magnetite, MLs at 200 and  $400 \mu\text{g Fe/mL}$  and liposome (adjust to MLs), after 24 h of incubation. The error bars indicate mean SEM. For the cell viability, relative values are given to those of control samples which not incubated with any particles but otherwise treated identically.

remarkably out-competed other targeting agents in some medical area.

### Ex Vivo Imaging

The magnetic resonance imaging of labeled cells (Fig. 7) confirmed the targeted and non-targeted iron uptake findings visually, it shows a clear generation of MR contrast of anti-HER2 VHH-MLs labeled HER2 positive cell lines as higher cell densities ( $1000 \text{ Cells}/\mu\text{L}$ ) lead to reduction in  $T_2/T_2^*$  relaxation times and a so called blooming effect in  $T_2^*$ -weighted MRI.  $T_2$ -weighted MR images allowed the visualization of the effect induced by MLs on the signal intensity of cell samples. Lower cell densities also led to appreciable MR contrast ( $200 \text{ Cells}/\mu\text{L}$ ) and even at the lowest density, dark spots corresponding to labeled cells were still detectable. Whiles, MR contrast of non-targeted MLs or magnetite at HER2 positive and HER2 negative cell lines have no significant difference.

## DISCUSSION

The main objective of this study was to assess the *in vitro* effect of targeted MLs by anti-HER2 VHH in compared to non-functionalized control MLs and magnetite using *in vitro* MRI and cell staining. The hypothesis was that targeted MLs could bind and internalized by receptor dependent way on the HER2 positive breast cancer cell line membrane for intellectual imaging. To date, USPIOs have frequently been used as MRI contrast agents and cell labeling tools for further MRI follow-up of the cells after transplantation *in vivo*.<sup>6,23</sup> By merging liposomes and USPIOs,

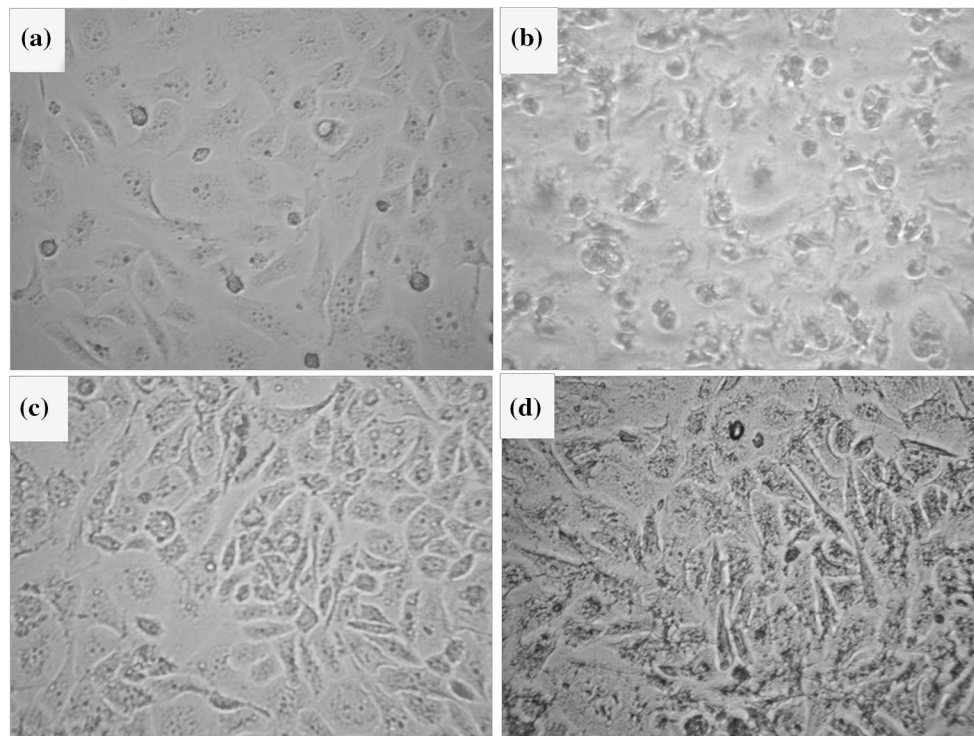


**FIGURE 5.** Visualization of cellular uptake of non-targeted magnetoliposome (a), magnetite (b), anti-HER2 VHH targeted ML (c) and Herceptin targeted ML (d) by Prussian blue staining of BT-474 after 8 h incubation.

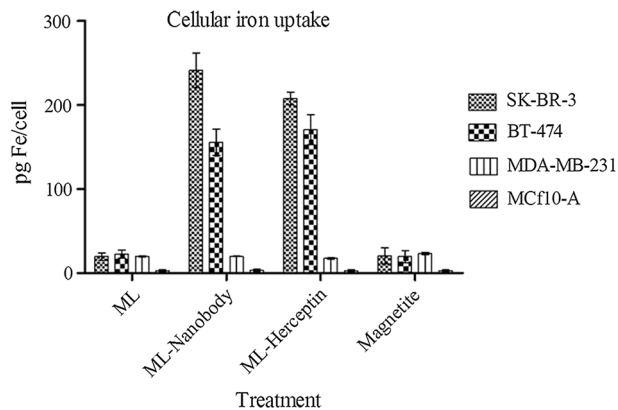


**FIGURE 6.** Intracellular iron content for HER2 positive (SK-BR-3 and BT-474), HER2 negative (MDA-MB-231) and normal breast cell line (MCF10-A) incubated with magnetite, non-targeted magnetoliposome, Herceptin targeted ML and anti-HER2 VHH targeted at 200  $\mu\text{g Fe/mL}$ , after 8 h of incubation. \* $p < 0.05$ ; \*\* $p < 0.01$ ; \*\*\* $p < 0.001$ .

MLs were borne, these creatures are potentially good multifunctional nanoplatforms for both imaging and chemotherapy.<sup>5,16</sup> Cancer cells often over express receptors for peptides, hormones and essential nutrients like iron or folic acid which provide an opportunity for the active and specific targeting of colloidal carriers.<sup>25</sup> Especially, HER1 and HER2, members of the human epidermal growth factor family of receptors

(HER), have been connected to 20–30% of breast cancer cases.<sup>7,14,25</sup>

In this study, we encapsulated a dextran coated USPIO in inert liposome to produce MLs by means of a double technique: first, the liposomes were prepared by reverse-phase evaporation using a suspension of ferrofluid as the aqueous medium. Then, the resulting liposomes were extruded through 100-nm pore membranes. After purification of MLs by Sepharose CL4B size exclusion chromatography column, a physicochemical characterization was performed, which included transmission electron microscopy, size distribution and stability assessment. Subsequently, the nanoparticles were targeted by anti-HER2 VHHs. Cytotoxicity assay was analyzed by PrestoBlue™ method on HER2 positive (BT-474, SK-BR-3), HER2 negative (MDA-MB-231) and normal breast (MCF10-A) cell lines. Cellular uptake was checked out in passive and active targeting by Prussian blue staining and optical microscopic assay. In previous study for gaining up the best ML with the most USPIO capacity and lowest cytotoxicity, encapsulation by several amount of USPIO was done. Furthermore the relaxivity measurement is done by several Fe concentrations.<sup>9</sup> Magnetite with coating by inert PEGylated liposomes has no cytotoxic effect on the cells during several time points and concentrations. Soenen *et al.* showed that the intracellular degradation of the con-



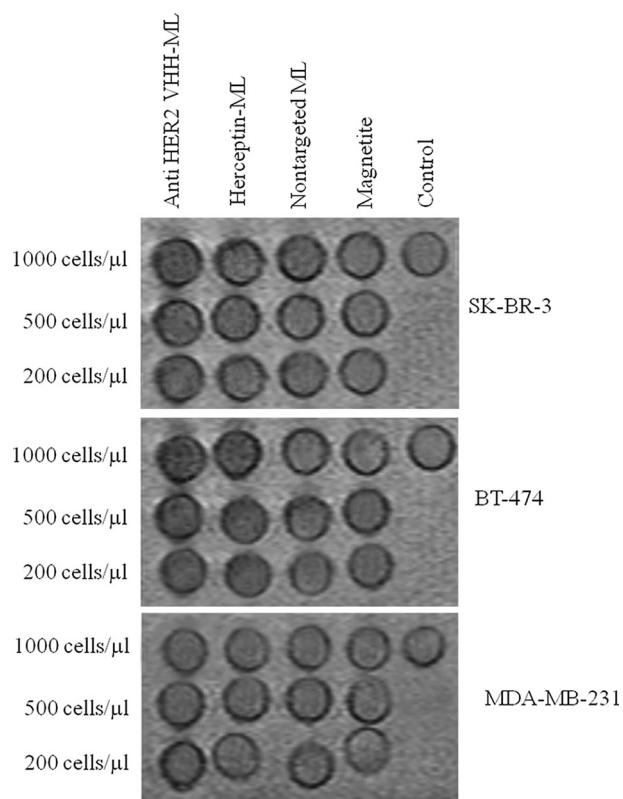


**FIGURE 7.** *Ex vivo* imaging. MR detection of magnetite (M), non-targeted magnetoliposome (ML), Herceptin targeted ML (HER2-ML) and anti-HER2 VHH targeted (VHH-ML) at 200 µg Fe/mL, after 8 h of incubation. Pictures show the presence of hypo-intense spots of magnetoliposomes and Magnetite, in 1.5 T MRI with cell densities of 1000, 500, 200 cells/µl of HER2 positive (SK-BR-3 and BT-474), HER2 negative (MDA-MB-231).

trast agent is an important issue and it was far more pronounced for magnetite nanoparticles like Sinerem<sup>®</sup> and far less for lipid-coated MLs. As a consequence, MLs have more stability on enduring endosomal degradation in compare to citrate- or dextran-coated particles so these compartments can be ideal CA for long-term detection of labeled cells, even upon recurrent cell divisions. The stability measurement shows that PEGylated and targeted MLs have enough stability during 4 weeks storage period in cell culture medium plus FBS, furthermore these kinds of MLs have enough stability in phosphate buffer saline during 4 weeks storage period.<sup>9</sup> The proteins of FBS can have effects on size and zeta potential which can interfere with cellular attachment and stability. So according to our results the differences in size and zeta potentials of samples in different concentrations of FBS were not significant and these showed our nano particles have suitable stability even in 10% FBS during 4 weeks storage. The stability of nano particles is a necessary characteristic for *in vivo* experiments; these results

show these kinds of magnetoliposomes may be stable in blood similar conditions. The coupling of anti-HER2 VHH to the surface of PEGylated MLs did not alter the specificity or inhibit the binding capacity of anti-HER2 VHH. Anti-HER2 VHH conjugated MLs (HER2-MLs) demonstrated specific binding to HER2 over expressing breast cancer cell lines (BT-474, SK-BR-3) as well as Herceptin conjugated MLs (Herceptin-MLs). However, the iron uptake outcomes show that anti-HER2 VHH-MLs have more ability to endocytose in compare with Herceptin-MLs despite of negative zetapotential after conjugation by VHH. It may be was due to small size and more penetration ability of VHHs into cells. Moreover, VHHs are smaller than antibodies and are thus more readily deliverable into cells also they have more stability in compare with whole antibodies. Of course the small sizes and high curvature angles of nanoparticles influence the types and amounts of proteins present on their surfaces. This differential display of proteins bound to the surface of NPs can influence the cellular uptake and biological effects of NPs.

Also, this finding was further strengthened when considering the *in vitro* MRI study. Our recent findings confirm that the amount of r2/r1 for all other samples including HER2 targeted ML, VHH targeted ML and non-targeted ML were between ~21 and ~28, which show the magnetite embedded samples have enough negative contrast to be detectable by magnetic resonance Imaging.<sup>9</sup> The magnetic resonance imaging of labeled cells confirmed the targeted and non-targeted iron uptake findings visually, it shows a clear generation of MR contrast of anti-HER2 VHH-MLs labeled HER2 positive cell lines as higher cell densities (1000 Cells/µL) lead to reduction in T2/T2\* relaxation times and a so called blooming effect in T2\*-weighted MRI. T2-weighted MR images allowed the visualization of the effect induced by MLs on the signal intensity of cell samples. Lower cell densities also led to appreciable MR contrast (200 Cells/µL) and even at the lowest density, dark spots corresponding to labeled cells were still detectable. Whiles, MR contrast of non-targeted MLs or magnetite at HER2 positive and HER2 negative cell lines have no significant difference.

We could assert these magic balls could target HER2 positive cell line effectively and MR contrast is detectable even by low cell densities. This intracellular clustering greatly enhances cell-associated MR contrast compared with common MR contrast agents and makes HER2-MLs interesting tools for efficient and long-term MR visualization of labeled cells and make anti-HER2 VHH-MLs perfect candidates to study the beginning stage of tumor formation and migration and homing of cancerous cells *in vivo*.



### CONFLICT OF INTEREST

The authors (Sepideh Khaleghi, Fatemeh Rahbarizadeh, Davoud Ahmadvand, Hamid Reza Madaah Hosseini) declare to have no competing interests.

### ETHICAL APPROVAL

This article does not contain any studies with human participants and animals performed by any of the authors.

### FUNDING

This paper was supported by Faculty of Medical Sciences, Tarbiat Modares University, Tehran, Iran and School of Allied Medical Sciences, Iran University of Medical Sciences, Tehran, Iran reference 16550.

### REFERENCES

- <sup>1</sup>Bonnet, C. S., Tóth É. MRI contrast agents. In: Ligand Design in Medicinal Inorganic Chemistry, 2014, pp. 321–354.
- <sup>2</sup>Clift, M. J., B. Rothen-Rutishauser, D. M. Brown, R. Duffin, K. Donaldson, L. Proudfoot, *et al.* The impact of different nanoparticle surface chemistry and size on uptake and toxicity in a murine macrophage cell line. *Toxicol. Appl. Pharmacol.* 232(3):418–427, 2008.
- <sup>3</sup>De Cuyper, M., S. J. Soenen, K. Coenegrachts, and L. T. Beek. Surface functionalization of magnetoliposomes in view of improving iron oxide-based magnetic resonance imaging contrast agents: anchoring of gadolinium ions to a lipophilic chelate. *Anal. Biochem.* 367(2):266–273, 2007.
- <sup>4</sup>De Meyer, T., S. Muyltermans, and A. Depicker. Nanobody-based products as research and diagnostic tools. *Trends Biotechnol.* 32(5):263–270, 2014.
- <sup>5</sup>Faria, M., M. Cruz, M. Gonçalves, A. Carvalho, G. Feio, and M. Martins. Synthesis and characterization of magnetoliposomes for MRI contrast enhancement. *Int. J. Pharm.* 446(1):183–190, 2013.
- <sup>6</sup>Frascione, D., C. Diwoy, G. Almer, P. Opriessnig, C. Vonach, K. Gradauer, *et al.* Ultrasmall superparamagnetic iron oxide (USPIO)-based liposomes as magnetic resonance imaging probes. *Int. J. Nanomed.* 7:2349, 2012.
- <sup>7</sup>Jamnani, F. R., F. Rahbarizadeh, M. A. Shokrgozar, D. Ahmadvand, F. Mahboudi, and Z. Sharifzadeh. Targeting high affinity and epitope-distinct oligoclonal nanobodies to HER2 over-expressing tumor cells. *Exp. Cell Res.* 318(10):1112–1124, 2012.
- <sup>8</sup>Jamnani, F. R., F. Rahbarizadeh, M. A. Shokrgozar, F. Mahboudi, D. Ahmadvand, Z. Sharifzadeh, *et al.* T cells expressing VHH-directed oligoclonal chimeric HER2 antigen receptors: towards tumor-directed oligoclonal T cell therapy. *Biochim. Biophys. Acta (BBA)-Gen. Subj.* 1840(1):378–386, 2014.
- <sup>9</sup>Khaleghi, S., F. Rahbarizadeh, D. Ahmadvand, M. Malek, and H. R. Madaah Hosseini. The effect of superparamagnetic iron oxide nanoparticles surface engineering on relaxivity of magnetoliposome. *Contrast Media Mol. Imaging* 11:340, 2016.
- <sup>10</sup>Lima-Tenório, M. K., E. A. G. Pineda, N. M. Ahmad, H. Fessi, and A. Elaissari. Magnetic nanoparticles: in vivo cancer diagnosis and therapy. *Int. J. Pharm.* 493(1):313–327, 2015.
- <sup>11</sup>Lu, R.-M., Y.-L. Chang, M.-S. Chen, and H.-C. Wu. Single chain anti-c-Met antibody conjugated nanoparticles for in vivo tumor-targeted imaging and drug delivery. *Biomaterials* 32(12):3265–3274, 2011.
- <sup>12</sup>Moghimi, S. M., F. Rahbarizadeh, D. Ahmadvand, and L. Parhamifar. Heavy chain only antibodies: a new paradigm in personalized HER2+ breast cancer therapy. *BioImpacts: BI* 3(1):1, 2013.
- <sup>13</sup>Oliveira, S., R. M. Schiffelers, J. van der Veecken, R. van der Meel, R. Vongpromek, P. M. V. B. en Henegouwen, *et al.* Downregulation of EGFR by a novel multivalent nanobody-liposome platform. *J. Control. Release* 145(2): 165–175, 2010.
- <sup>14</sup>Reynolds, J. G., E. Geretti, B. S. Hendriks, H. Lee, S. C. Leonard, S. G. Klinz, *et al.* HER2-targeted liposomal doxorubicin displays enhanced anti-tumorigenic effects without associated cardiotoxicity. *Toxicol. Appl. Pharmacol.* 262(1):1–10, 2012.
- <sup>15</sup>Rotman, M., M. M. Welling, A. Bunschoten, M. E. de Backer, J. Rip, R. J. Nabuurs, *et al.* Enhanced glutathione PEGylated liposomal brain delivery of an anti-amyloid single domain antibody fragment in a mouse model for Alzheimer's disease. *J. Control. Release* 203:40–50, 2015.
- <sup>16</sup>Sabaté, R., R. Barnadas-Rodríguez, J. Callejas-Fernández, R. Hidalgo-Álvarez, and J. Estelrich. Preparation and characterization of extruded magnetoliposomes. *Int. J. Pharm.* 347(1):156–162, 2008.
- <sup>17</sup>Sadeqzadeh, E., F. Rahbarizadeh, D. Ahmadvand, M. J. Rasaei, L. Parhamifar, and S. M. Moghimi. Combined MUC1-specific nanobody-tagged PEG-polyethylenimine polyplex targeting and transcriptional targeting of tBid transgene for directed killing of MUC1 over-expressing tumour cells. *J. Control. Release* 156(1):85–91, 2011.
- <sup>18</sup>Sharifzadeh, Z., F. Rahbarizadeh, M. A. Shokrgozar, D. Ahmadvand, F. Mahboudi, F. R. Jamnani, *et al.* Genetically engineered T cells bearing chimeric nanoconstructed receptors harboring TAG-72-specific camelid single domain antibodies as targeting agents. *Cancer Lett.* 334(2):237–244, 2013.
- <sup>19</sup>Shinkai, M., M. Suzuki, S. Iijima, and T. Kobayashi. Antibody-conjugated magnetoliposomes for targeting cancer cells and their application in hyperthermia. *Biotechnol. Appl. Biochem.* 21(2):125–137, 1995.
- <sup>20</sup>Singh, A., and S. K. Sahoo. Magnetic nanoparticles: a novel platform for cancer theranostics. *Drug Discov. Today* 19(4):474–481, 2014.
- <sup>21</sup>Soenen, S. J., J. Baert, and M. De Cuyper. Optimal conditions for labelling of 3T3 fibroblasts with magnetoliposomes without affecting cellular viability. *Chembiochem* 8(17):2067–2077, 2007.
- <sup>22</sup>Soenen, S. J., M. De Cuyper, S. C. De Smedt, and K. Braeckmans. Investigating the toxic effects of iron oxide nanoparticles. *Methods Enzymol.* 509:195–224, 2012.
- <sup>23</sup>Soenen, S. J., S. F. De Meyer, T. Dresselaers, G. V. Velde, I. M. Pareyn, K. Braeckmans, *et al.* MRI assessment of blood outgrowth endothelial cell homing using cationic magnetoliposomes. *Biomaterials* 32(17):4140–4150, 2011.
- <sup>24</sup>Soenen, S. J., G. V. Velde, A. Ketkar-Atre, U. Himmelreich, and M. De Cuyper. Magnetoliposomes as magnetic

- resonance imaging contrast agents. *Wiley Interdiscip. Rev.: Nanomed. Nanobiotechnol.* 3(2):197–211, 2011.
- <sup>25</sup>Steinhauser, I., B. Spänkuch, K. Strebhardt, and K. Langer. Trastuzumab-modified nanoparticles: optimisation of preparation and uptake in cancer cells. *Biomaterials* 27(28):4975–4983, 2006.
- <sup>26</sup>Van de Broek, B., N. Devoogdt, A. D'Hollander, H.-L. Gijs, K. Jans, L. Lagae, *et al.* Specific cell targeting with nanobody conjugated branched gold nanoparticles for photothermal therapy. *ACS Nano* 5(6):4319–4328, 2011.
- <sup>27</sup>Wray, W., T. Boulikas, V. P. Wray, and R. Hancock. Silver staining of proteins in polyacrylamide gels. *Anal. Biochem.* 118(1):197–203, 1981.
- <sup>28</sup>Yigit, M. V., A. Moore, and Z. Medarova. Magnetic nanoparticles for cancer diagnosis and therapy. *Pharm. Res.* 29(5):1180–1188, 2012.